

1 **Method and Apparatus for Removing Orbital Space Debris from Near Earth Orbit Using the**
2 **Solar Wind: Platform for Redirecting and Removing Inert Space Material (PRRISM)**

3 **John F Dargin III**

4 Ironstar Engineering, LLC, 56 Depot Street #2221, Duxbury, Massachusetts 02331 USA,
5 ian@ironstarengineering.com

6
7 **ABSTRACT**

8
9 A Platform for Redirecting and Removing Inert Space Material (PRRISM) is a system utilizing an antenna generating
10 an electromagnetic (EM) wave to interact with a solar EM wave to streamline magnetic flux in the Polar Cusp and to
11 facilitate the flow of solar plasma through the Polar Cusp, resulting in an increased density, velocity, and pressure at
12 the exit of the Polar Cusp. The elevated plasma flow intercepts and removes small space debris from Low Earth Orbit
13 (LEO), Geosynchronous Earth Orbit (GEO) and Geosynchronous Transfer Orbits (GTO) transiting the LEO altitude
14 regimes. Patent: US 10,501,212 B2, Dated: December 10, 2019

15
16 **1 INTRODUCTION**

17
18 There have been numerous articles and technical papers on the dangers of operating in Low Earth Orbit (LEO) at
19 altitudes between 160 km and 2000 km (0.03 – 0.3 R_E) with the threat of collision with countless small and large
20 orbital debris. This debris occupies LEO and extends out to Geostationary Earth Orbit or Geosynchronous Earth Orbit
21 (GEO) at a circular orbit of 35,786 km (5.6 R_E) above the Earth's equator. There are various inclinations and altitudes
22 defining operational satellite orbits in proximity with a multitude of space debris. This space junk is comprised of
23 derelict satellites, rocket bodies, and metal fragments from explosions or collisions. There are many other numerous
24 small detectable or in many cases undetectable particles such as nuts, bolts, paint chips, gloves, etc. Tracking of the
25 space debris is currently managed by the Air Force Joint Space Operations Center (JSpOC). The JSpOC monitors
26 space debris greater than 10 cm in diameter and is currently tracking more than 8,500 objects. Estimates on the amount
27 of debris less than 10 cm, range from 500,000 and up.

28
29
30
31
32
33
34
35
36
37
38
39
40
41
42
43
44
45
46
47
48
49
50
51
52
53
54
55
56

2 STUDIES

Space debris de-orbits over time due to increased drag forces as the orbital velocity of the debris slowly decays with increasing contact with the Earth's upper atmosphere. This takes many months or years and studies have shown that natural decay will not keep pace with the growing amount of space debris. In fact, we may be reaching a point where additional debris will result in a cascading effect of collisions generating more debris. There are numerous examples of high-speed collisions in low Earth orbit between satellites and with the space shuttle. A study initiated via a United Nations Inter-Agency Space Debris Coordination Committee (IADC) Action Item 27.1, Stability of the Future LEO Environment, was conducted by six IADC member agencies to investigate the projected growth of the LEO debris population. Each concluded independently that active satellite management and debris removal, including the 25-year rule, is necessary to prevent collisions in the future. [1]

2.1 Kessler Syndrome

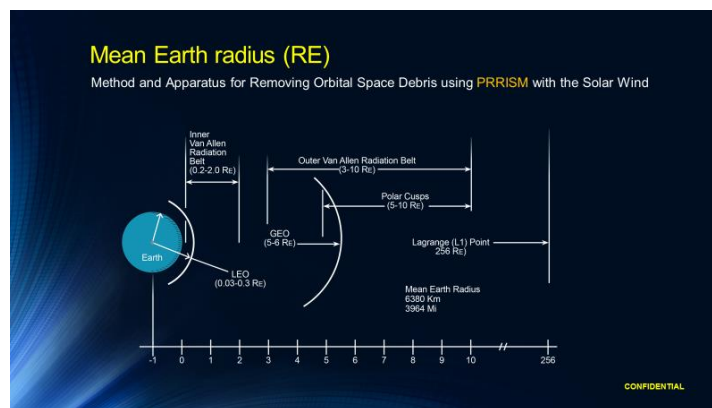
The Kessler Syndrome [2] which helps to explain these phenomena is defined as the numerical growth of satellites and other space objects in orbit to a point where a collision with space debris will generate more debris particles which will then result in more collisions and so on until near Earth orbit becomes unusable. Except for PRRISM, the orbital space debris removal techniques to date have involved the use of a Satellite for delivery of a device or material and are required to operate in the same orbits as the debris. Some of these concepts include a collecting device or net for small debris, a tether or grappling device for larger objects, a laser beam targeting system, a dust injection system, or atmospheric gas injection system. Many involve high mass and energy systems that would contribute to the existing debris and become part of the problem.

57 **3 ORBITS**

58

59 The Low Earth Orbit (LEO) is defined as an altitude less than 2000 km with the most concentrated altitudes ranging
60 from 450km to 1000km [3]. Within the LEO altitude range are many satellites having inclinations crossing near the
61 poles between 80° and 110°. Within a tighter band, are the more concentrated satellites in a Sun Synchronous Orbit
62 (SSO) with inclinations between 96.5° and 102.5° [4,5]. A SSO (also called a helio-synchronous orbit), as defined by
63 Wikipedia, is a geocentric orbit that combines altitude and inclination in such a way that the satellite passes over any
64 given point of the planet's surface at the same local solar time. Other satellites operate at various inclinations from
65 equatorial to polar to retrograde (inclination angle is greater than 90°) and range from circular (eccentricity = 0) to
66 highly elliptical (eccentricity greater than zero and less than one). Debris fields in elliptical orbits would have a Perigee
67 altitude within the LEO altitude range and Apogee well above LEO. There are currently over 20,000 satellites
68 operating between LEO and Geosynchronous Earth Orbit (GEO) with inclinations ranging from equatorial or 0° to
69 polar at 90° and up to 110°. The GEO is defined as an altitude range between 32,000 km and 37,000 km and a near
70 circular orbit. On a larger scale, distances can be given as a multiple of the Mean Earth Radius (R_E), where 1 R_E = 6380
71 km. Figure 1 presents a sketch of various near-Earth locations measured in R_E to show relative distance in the near-
72 Earth environment.

73



74

75

76

77

78

79

Fig. 1 Mean Earth Radius

80 **4 SOLAR WIND**

81

82 Scientific studies of the solar plasma emanating from the sun have shown that the flow spirals outward from the sun in
83 a flow pattern illustrated in Fig. 2, which is often referred to as the “Parker Spiral,” at two distinct speeds and with an
84 electrical charge distributed in a toroidal wave that reaches the Earth with a balanced electrical charge. The
85 solar plasma is composed of 96% protons, 4% He+ ions, minor constituents plus an adequate number of electrons for a
86 balanced charge [6]. Within the solar wind is contained the solar plasma of electrically charged particles (E field) and
87 the interplanetary magnetic field (IMF) or B field, which are mutually perpendicular and perpendicular to the direction
88 of flow. However, the solar wind and the solar plasma terms may be used interchangeably throughout this Paper.

89 Alfvén waves (a type of magnetohydrodynamic wave) embedded within the high-speed solar plasma have a wide range
90 of periods/frequencies. Only those with periods longer than 8 minutes can affect the oral regions of the Earth (where
91 the Aurora Borealis is generated) [7]. The slow solar wind speed has been recorded at 350 km/s originating from the
92 Sun’s equatorial region, while the high-speed wind has been estimated at 800 km/s and emanating from the solar polar
93 regions at latitudes above 30°. These plasma dense current sheets have been recorded with stronger polar magnetic
94 fields and redistributed as the solar wind flows outward, reportedly achieving a near uniform magnetic field
95 distribution by about five solar radii. Solar cycles with Coronal Mass Ejection (CME) activity will likely affect solar
96 wind speed, magnetic field, and electrical charge. CME can be defined as a giant cloud of solar plasma drenched with
97 magnetic field lines that are blown away from the Sun during strong, long-duration solar flares and filament eruptions.

98

99



100

101

102

Fig. 2 Parker Spiral

103
104
105
106
107
108
109
110
111
112
113
114
115
116
117
118
119
120
121
122
123
124
125
126
127
128
129
130
131

5 ELECTROMAGNETIC WAVES

We also know from Maxwell's equations that a changing electrical field produces a magnetic field and a changing magnetic field produces an electrical field. Further, accelerating electric charges generate electromagnetic waves. Data from the Hawkeye science mission were recorded during polar cusp crossings of between 5 to 10 R_E at the northern cusp and between 1.1 and 2.0 R_E for the southern cusp. The ULF-ELF magnetic field noise from about 1.78 to 178 kHz is the primary plasma wave phenomena and a reliable indication of the polar cusp [8]. Contained within the solar wind are both electrical and magnetic fields. The changing electrical field along with the changing magnetic field contributes to the strong electromagnetic wave moving outward from the Sun at the two distinct speeds of 350 km/sec and 800 km/sec. As this EM wave approaches the Earth's geomagnetic field, a strong reconnection process occurs that disturbs the flow and reduces energy levels within the polar cusp. Hawkeye measurements of the electric field within the polar cusp revealed values of 1 to 5 mV per meter. In contrast, an electric field measurement of the free stream solar wind upstream of Earth is 1×10^3 V per meter. The following pages will show that a measured force with constructive interference is required to resonate with the electromagnetic field in the polar cusp to reduce turbulence, allowing an increase in the force producing laminar flow to intercept with the targeted debris. A means of frequency matching and pulsing of the EM wave with a parabolic antenna to achieve laminar flow through the Polar Cusp is necessary to improve the flow rate and ultimately the force output from the polar Cusp. Using the source-free Maxwell's equations [9].

$$\nabla_{\times} E = - \partial B / \partial t \quad \text{for a changing magnetic field} \quad \text{Eq. 1}$$

$$\nabla_{\times} H = \partial D / \partial t \quad \text{for a changing electrical field} \quad \text{Eq. 2}$$

where E and H are the electric and magnetic field intensities, measured in units of volts/m and amperes/m, respectively; D and B are the electric and magnetic flux densities and are in units of coulomb/ m^2 and weber/ m^2 respectively.

132 The force on a charge q moving with velocity v in the presence of an electric field E and a magnetic field B is called
133 the Lorentz force and is given by:

$$134 \quad F = q (E + v \times B) \quad \text{Eq. 3}$$

135
136 For an electromagnetic wave moving through a vacuum, the constitutive relation of the electric and magnetic flux
137 densities D , B are related to the field intensities E , H in the simplest form:

$$138 \quad D = \epsilon_0 E \quad \text{and} \quad B = \mu_0 H \quad \text{Eqs. 4 and 5}$$

139
140
141 where ϵ_0 and μ_0 are the permittivity and permeability of vacuum with numerical values:

$$142 \quad \epsilon_0 = 8.854 \times 10^{-12} \text{ farad/ m}$$

$$143 \quad \mu_0 = 4 \pi \times 10^{-7} \text{ henry/ m}$$

144

145

146

147 **5.1 EM Waves**

148

149 Accordingly, the net force on a moving charge exerted by a time-varying electromagnetic (EM) field is proportional to
150 the magnitude and polarity of the charge, the velocity of the charge, the magnitude, direction and polarization of the
151 EM field, and the frequency of the EM field. These principles are used to focus and accelerate charged particles in
152 particle accelerators such as linear accelerators and cyclotrons. The EM field parameters required to manipulate a
153 specific charge (a solar plasma ion or electron) can be determined by closed form calculation, multi-physics finite
154 element modeling, or by experimentation. While charged plasma particles might have a bearing on eliminating
155 turbulence within the polar cusp, it is also noted that the interplanetary magnetic field (IMF) fluctuations are more
156 important than the variations in the solar wind speed for transferring energy into the polar cusp [7]. In another paper,
157 the solar wind is described as "magnetic spaghetti" where the magnetic flux tubes are surrounded by electrically
158 charged sheets of solar plasma with thicknesses of 1000 to 2000 km [10]. These magnetic flux tubes can be from 35
159 R_E up to and greater than 100 R_E in diameter and are oriented with the Parker spiral at about a 45° angle to the Sun -

160 Earth line. Furthermore, it can take about 20 minutes for one magnetic flux tube to interact with the Earth's
 161 geomagnetic field before a 2nd flux tube arrives with possibly a different set of electromagnetic parameters.

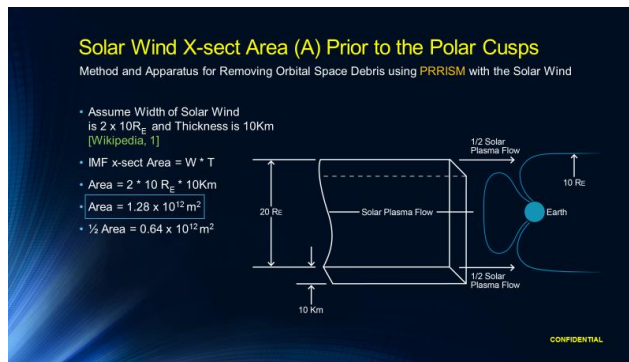
162

163 **6 FREESTREAM SOLAR WIND CALCULATIONS**

164

165 Now we calculate the unimpeded free-stream solar wind mass flow, dynamic pressure, and force to determine the
 166 pressure force that could be available to provide sufficient force to remove space debris from low Earth orbit. First,
 167 looking at the solar wind mass flow, we take the cross-sectional area of the IMF as in Fig. 3. Using 10 km as the
 168 thickness per Wikipedia and then taking the width as 2 x 10 R_E, with 1R_E = 6380 km we have the Area as:

169



170

171

172 Fig. 3 Solar Wind Free stream

173

174
$$\text{Area} = 2 * 10 R_E * 10 \text{ km} \tag{Eq. 6}$$

175

176
$$\text{Area} = 1.28 * 10^{12} \text{ m}^2$$

177

178 Solving for the Mass flow: $(M) = \rho * A * v_p \tag{Eq. 7}$

179

180 where $\rho = \text{proton mass } (m_p) \text{ kg} * \text{protons } (n_p) \text{ cm}^{-3}$

181
$$m_p = 1.673 * 10^{-27} \text{ kg} \text{ and } n_p = 9 \text{ cm}^{-3}$$

182 $A = \text{cross section Area of the freestream solar wind} = 1.28 * 10^{12} \text{ m}^2$

183 $v_p = \text{slower solar wind speed} = 350 \text{ km/ sec}$

184 $M = 6.76 \times 10^{-3} \text{ kg/sec}$

185

186 The Dynamic Press (P) = $m_p * n_p * v_p^2$ Eq. 8

187

188 $P = 1.673 \times 10^{-27} \text{ kg} * 9 \times 10^6 / \text{m}^3 * 1.225 \times 10^{11} \text{ m}^2 / \text{sec}^2$

189

$P = 1.84 \text{ nPa}$

190

191

192

193 The Free-stream Solar Wind Force (F) = Dynamic Pressure (P) * Area (A) Eq. 9

194

195

$F = 2360 \text{ Newtons}$

196

197 **7 POLAR CUSP CHARACTERISTICS**

198

199 As the solar wind approaches the Polar Cusps, observations from the IMP - 8 and Hawkeye satellites have shown that

200 there are two significant areas defining the Polar Cusp: the external Polar Cusp area and the internal Polar Cusp area.

201 Figure 4 illustrates the exterior and interior areas of the Polar Cusp with respect to the magnetosheath and the

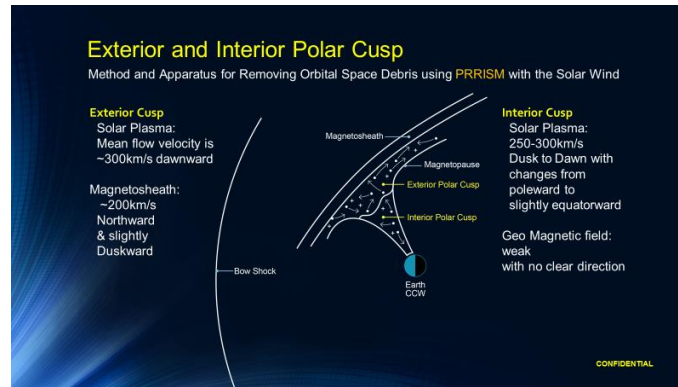
202 magnetopause. The Earth's rotation is counterclockwise so that the dawn to dusk flow would be out of the paper and

203 the dusk to dawn flow would be into the paper. In the vicinity of the exterior of the Polar Cusp, the solar wind,

204 flowing with both the charged particles of the solar plasma and the interplanetary magnetic field (IMF), interact with

205 the Earth's geomagnetic field and begin a complex reconnection process with significant turbulence [11].

206



207

208

209

Fig. 4 Polar Cusp Environment

210 7.1 Hawkeye Data

211

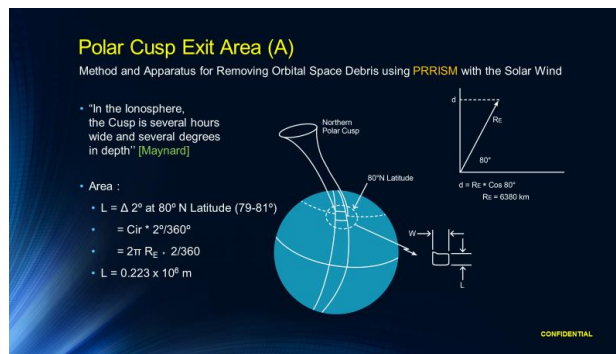
212 Hawkeye plasma, magnetic field, and plasma wave instruments have directly sampled the throat of the northern Polar
 213 Cusp. The interplanetary magnetic field was observed to change from Southward to Northward on July 3, 1974. There
 214 were 2 distinct regions identified based on magnetic field plasma flow and magnetic and electric noise. Based on the
 215 data, the dominant factor determining the initial location of reconnection and evolution of the reconnected flux is the
 216 orientation of the IMF. The IMF orientation (Southward or Northward) at the magnetopause is more important than
 217 variations in solar wind speed for setting the initial location for flux tube reconnection [11]. It is important to note that
 218 as the density in the Polar Cusp increases, the greater the force will be on the space debris. In addition, the solar wind
 219 Alfvén waves within the Parker spiral affect the magnetospheric dayside cusp density and heat the cusp [7]. The
 220 proton density in the solar plasma is unchanged at 9 per cubic centimeter until below 4 R_E when the density increases
 221 deeper into the cusp [11]. Furthermore, the energetic population within the Cusp is composed of both ionospheric (O^+)
 222 ions, and solar wind (He^{++} , $O^{>+3}$). The presence of ionospheric ions higher in the Polar Cusp with some vertical flow
 223 indicates the presence of a turbulent region within the Polar Cusp. It was observed that the flow in the exterior and
 224 interior Polar Cusp is turbulent. In the exterior cusp, the mean flow velocity is 300 km/s downward (Earth's rotation is
 225 counterclockwise as indicated in Fig. 4), whereas, the Magnetosheath flow is 200 km/s Northward. In the interior
 226 cusp, the solar plasma is 250-300 km/s dusk to dawn with slight direction changes from poleward to the equator and
 227 the geomagnetic field is weak. Hence, the data shows that within the exterior cusp, the magnetic field components
 228 change from those in the Magnetosheath and become more variable. Once entering the Cusp, the bulk flow becomes
 229 disturbed from the steadier flow in the Magnetosheath.

230 **7.2 Polar Cusp Exit Calculations**

231

232 The calculation for the normal solar wind flow exiting the Polar Cusps requires estimates for calculating the Mass flow
 233 (M), Dynamic Pressure (P) and Solar Wind Force (F) that could be applied against the targeted debris in Low Earth
 234 Orbit. As shown in Fig. 5, “In the Ionosphere the cusp is several hours wide and several degrees in depth” [12,13], the
 235 exit area of the Cusp would be represented by length (L) of 2° of north latitude from 79° to 81°. The width (W) would
 236 be 2/ 24 hours on the circumference at 80° north latitude. Therefore:

237



238

239

Fig. 5 Polar Cusp Exit Area

240

241

242

$$\text{Area} = L * W$$

Eq. 10

243

244

$$L = \Delta 2^\circ \text{ at } 80^\circ \text{ N Latitude } (79^\circ-81^\circ) \text{ where } R_E = 6380 \text{ km,}$$

245

$$= \text{Cir} * (2^\circ / 360^\circ)$$

246

$$= 2 \Pi R_E * 10^6 \text{ m} * (2^\circ / 360^\circ)$$

247

$$L = 0.223 \times 10^6 \text{ m}$$

248

$$W = 2/ 24 \text{ hours at } 80^\circ \text{ North Latitude}$$

249

$$= (2/ 24) * 2 \Pi R_E \text{ Cos } 80^\circ$$

250

$$W = 0.580 \times 10^6 \text{ m}$$

251

$$\text{Area} = 0.223 \times 10^6 \text{ m} * 0.580 \times 10^6 \text{ m}$$

252

$$\text{Area of the Cusp exit (A)} = 0.129 \times 10^{12} \text{ m}^2$$

253

254 The Mass flow (M) is calculated with the following values:

255

$$256 \quad M = \rho * A * v \quad \text{Eq. 11}$$

257

$$258 \quad \text{Where } \rho = m_p * n_p$$

$$259 \quad m_p = 1.673 \times 10^{-27} \text{ kg; mass of a proton}$$

$$260 \quad n_p = 15 \text{ cm}^{-3}; \text{ number concentration of protons}$$

$$261 \quad \text{Area} = 0.129 \times 10^{12} \text{ m}^2$$

$$262 \quad \text{Velocity (v)} = 100 \text{ km/ sec}$$

$$263 \quad M_{\text{cusp}} = 1.673 \times 10^{-27} \text{ kg} * 15 \text{ cm}^{-3} * 0.129 \times 10^{12} \text{ m}^2 * 100 \text{ km/ sec}$$

$$264 \quad \text{The Mass flow at the Cusp Exit is: } M = 0.324 \times 10^{-3} \text{ kg/sec}$$

265 The Dynamic Pressure (P) through the Polar Cusp:

266

$$267 \quad P = m_p * n_p * v_p^2 \quad \text{Eq. 12}$$

268

$$269 \quad \text{where } m_p = 1.673 \times 10^{-27}$$

$$270 \quad n_p = 15 \text{ cm}^{-3}$$

$$271 \quad v_p = 100 \text{ km/ sec}$$

$$272 \quad P = 1.673 \times 10^{-27} \text{ kg} * 15 \text{ cm}^{-3} * (100 \text{ km/sec})^2$$

$$273 \quad P = 0.251 \times 10^{-9} \text{ kg/m-sec}^2$$

$$274 \quad \text{The Dynamic Pressure (P) at the Cusp Exit is: } P = 0.251 \text{ nPa}$$

275

276 The Estimated Normal Solar Wind Force (F) at the Cusp exit is:

277

$$278 \quad F = \text{Dynamic Pressure (P)} * \text{Area of the Cusp Exit (A)} \quad \text{Eq. 13}$$

279

$$280 \quad P = 0.251 \times 10^{-9} \text{ kg/m-sec}^2$$

$$281 \quad A = 0.129 \times 10^{12} \text{ m}^2$$

$$282 \quad F = (0.251 \times 10^{-9} \text{ kg/m-sec}^2) * (0.129 \times 10^{12} \text{ m}^2)$$

283 $= 0.0324 \times 10^3 \text{ kg} - \text{m/ sec}^2$

284 The Estimated Normal Solar Wind Force (F) at the Cusp exit is:

285 $F = 32.4 \text{ Newtons}$

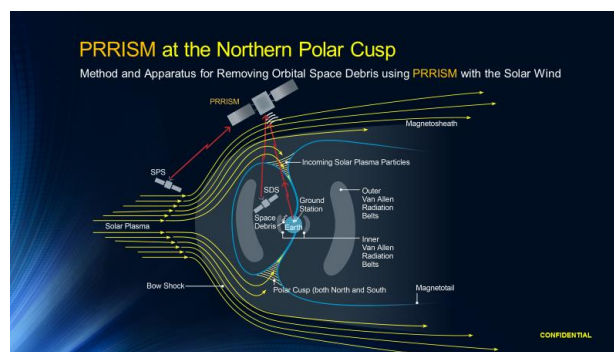
286

287 7.3 Polar Cusp and EM Wave Effect

288

289 While the North and South poles offer a natural magnetic attraction for the solar wind and the highly charged plasma
290 particles, the solar wind offers a readily available medium to help sweep away the small debris particles in Low Earth
291 Orbit. As illustrated in Fig. 6, PRRISM would use an electromagnetic wave generated by an antenna mounted on a
292 dedicated satellite and placed in a $10R_E$ elliptical orbit above and near the intercept at the Polar Cusps, or at some other
293 optimum location. The PRRISM satellite, would aim electromagnetic waves into the Polar Cusp to reduce turbulence,
294 increase the density, redirect and streamline the particle flow within the cusp and increase the temperature and density
295 so that a greater pressure force could be directed onto the space debris. The charged particles present in the high
296 velocity flow of the solar wind are naturally redirected through the Polar Cusp with an antenna-focused
297 electromagnetic wave. Using the electromagnetic wave, the naturally diverted solar wind flow could be strengthened
298 by improving the laminar flow, reducing turbulence, and increasing the density by heating the plasma through the Polar
299 Cusp. This highly charged flow of solar wind could be harnessed and regulated to induce a discrete pressure wave burst
300 of plasma at a specific time and duration (per a computer-generated target solution) when the debris cloud is passing
301 below the Polar Cusps near the North or South pole.

302



303

304

305

Fig. 6. Northern Polar Cusp

306

307 **8 INTERCEPT CALCULATION**

308

309 Figure 7 illustrates a 2-D computation for an intercept with the solar wind flow and the space debris in either Low
310 Earth or Geosynchronous Earth Orbit. A more rigorous 3-D calculation could be accomplished using a computer
311 program to develop the solutions using a "quartic formula". In this figure, PRRISM is located at an estimated location
312 of 10 R_E and the target space debris located in a Low Earth orbit of 0.2 R_E. Assuming constant velocity, an estimate of
313 the time to intercept can be determined by using the formula:

314

315
$$t = d/v$$
 Eq. 14

316

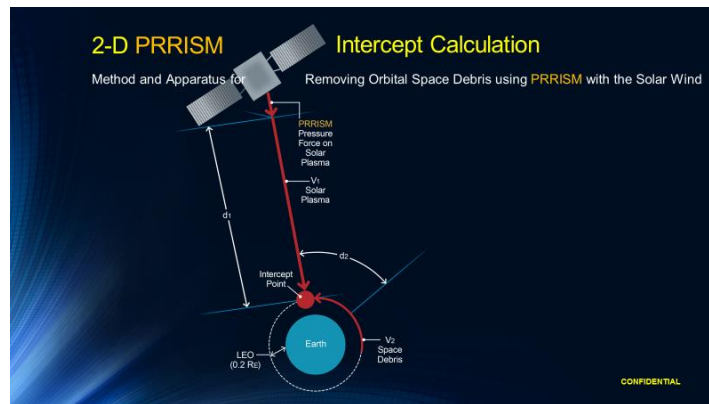
317 where: t is the time to intercept

318 d is the distance traveled

319 v is the velocity

320

321



322

323

324 Fig. 7 2-D Intercept calculation

325

326 For the intercept to occur, the time t_1 for the diverted plasma flow must equal the time t_2 for the space debris.

327 This results in the formula: $d_1/v_1 = d_2/v_2$.

328 Using $d_1 = 9.8 R_E$

329 $v_1 = 350$ km/s for the solar plasma and

330 $t_1 = t_2$ With $R_E = 6380$ km and solving for t_1

331 Yields $t_1 = 178.6$ sec

332 This is just under 3 minutes to the intercept location and contact with the debris. At this point the debris velocity
333 would decrease, causing the debris to move into a lower and decaying orbit by using the higher-pressure force of the
334 diverted and more laminar solar plasma flow. Variations of this diverted solar plasma flow would be to use a
335 larger/stronger EM wave or multiple PRRISM satellites. The process would be repeated as each debris cloud passes
336 into the target area and the plasma flow would be redirected with a sufficient mass flow to intercept and remove the
337 debris into a deteriorating orbit to burn up harmlessly in the Earth's atmosphere.

338

339 **9 DEBRIS CALCULATIONS**

340

341 Several calculations were made to determine the force required to cause a piece of space debris in a 500km orbit to de-
342 orbit. First, the mass of a small piece of space debris is calculated. D. Kessler [2] determined that the average mass
343 density (ρ) for debris objects 1 cm in diameter and smaller is 2.8 g/cm^3 . For debris larger than 1 cm:

344

$$345 \rho = 2.8 d^{-0.74} \quad \text{Eq. 15}$$

346

347 For a diameter (d) of 2 cm, which is the smallest detectable size, the mass density is:

$$348 \rho = 2.8 * (2)^{-0.74}$$

$$349 = 1.68 \text{ g/cm}^3$$

350

$$351 \text{ The mass of a 2-cm piece of space debris: } m = \rho * 4/3 * \pi * r^3 \quad \text{Eq. 16}$$

352

$$353 m = 7 \text{ g}$$

354

355 The force necessary to keep a small mass of space debris in a 500-km orbit is shown by this relationship:

356

$$357 \text{ Force}_{\text{Space Debris}} = G (M_E * m_{SD}) / r_{SD}^2 \quad \text{Eq. 17}$$

358

359 where: $G = \text{Gravitational constant} = 6.67 \times 10^{-11} \text{N-m}^2 / \text{kg}^2$

360 $M_E = \text{Mass of Earth} = 5.98 \times 10^{24} \text{ kg}$

361 $m_{SD} = \text{mass of space debris} = 7 \times 10^{-3} \text{ kg}$

362 $r_{SD} = \text{radial distance to the debris orbit} = 6380 \text{ km} + 500 \text{ km} = 6880 \text{ km}$

363 $\text{Force}_{\text{Space Debris}} = 6.67 \times 10^{-11} \text{N-m}^2 / \text{kg}^2 * (5.98 \times 10^{24} \text{ kg} * 7 \times 10^{-3} \text{ kg}) / (6.88 \times 10^6 \text{ m})^2$

364 $\text{Force}_{\text{Space Debris}} = 0.059 \text{ Newtons}$

365

366 $\text{Force to remove 2 cm debris} > 0.059 \text{ Newtons}$

367

368 Hence, a force greater than 0.059 Newtons would remove a piece of Space debris 2-cm in diameter from a 500-km
369 orbit. For an orbit of 1000 km, the force is slightly less at 0.051 Newtons. A mass that represents a 2-cm diameter
370 piece of debris was used based on Dr. Kessler's equation which was developed from numerous catalogued debris of
371 different sizes and materials [2]. As can be seen from earlier calculations, the estimated pressure force of the normal
372 solar wind flow of 32.4 Newtons was calculated through the Polar Cusp and would be sufficient, if unimpeded, to
373 remove this and other small pieces of debris. However, space science data has shown that the turbulence in the Polar
374 Cusp reduces the downward flow of the solar plasma in such a way that this pressure force is never achieved. By
375 creating a laminar flow in the Polar Cusp, a pressure force greater than 32.4 Newtons can be obtained.

376

377 **10 PRRISM OPERATION**

378

379 Previous solar science missions were placed in many different orbits with slightly different objectives but using a
380 variety of science instruments with some overlap in objectives and methodology. The WIND Satellite operated in a
381 halo orbit about the L1 Lagrange point at 256 R_E ; the Hawkeye Satellite was in an elliptical orbit with an apogee of
382 21 R_E , passing through the northern cusp at 5 to 10 R_E ; and the Polar Satellite was in an elliptical polar orbit of 9.5 R_E x
383 1.8 R_E . The PRRISM satellite, located in a 10 R_E elliptical orbit above the Polar Cusp and outside the target orbits,
384 would receive telemetry data from the Solar Plasma Sensor (SPS), either on board or remotely located upstream of the
385 Polar Cusp and from the Space Debris Sensor (SDS), also on board or remotely located. A variety of instruments have
386 been used on earlier space science missions and can be modified as necessary to meet mission requirements for the

387 Solar Plasma Sensor as well as the Space Debris Sensor. The Targeting Computer (TC) on board the PRRISM Satellite
388 would receive the telemetry data from the SPS regarding the plasma polarity, plasma electrical charge, plasma
389 magnetic field strength, electron density, ion density, proton density, flux density, frequency and velocity of the solar
390 plasma. The SDS would send telemetry data to the TC with debris data such as density, size, velocity, and orbit
391 parameters of the debris cloud passing beneath the Polar Cusps. The TC would then determine the required orientation
392 of the PRRISM antenna, the magnitude, frequency, and polarization of the electromagnetic wave, along with the timing
393 and power-up sequencing of the PRRISM antenna. This electromagnetic wave antenna would then aim a narrow beam
394 into the Polar Cusp to decrease turbulence and increase the laminar flow of the plasma through the Polar Cusp while
395 increasing the temperature and proton density within the plasma. The TC would also provide intercept coordinates and
396 duration for the electromagnetic directed pressure wave of solar plasma to intercept and move the debris cloud into a
397 decaying orbit. The result would be to redirect the debris into the atmosphere to burn up along with other charged
398 plasma creating the familiar light show known as the northern and southern lights. The timing and sequencing of the
399 electromagnetic (EM) wave could be pulsed or varied depending on the pressure force required.

400

401 **10.1 PRRISM SYSTEMS**

402

403 The primary PRRISM satellite systems are the following: The Satellite Telemetry, Tracking & Control Subsystem
404 (TTCS) provides the capability to command and operate the Satellite and to receive, record and transmit science and
405 engineering telemetry data. This unit can execute commands in real time or storing them for delayed execution. The
406 Satellite Electrical Power Distribution Subsystem (EPDS) provides for the generation, storage, distribution, and control
407 of power required for operating the Satellite and instruments. While sunlit, power is normally supplied by the solar
408 arrays. The Batteries supply power while in the Earth's shadow, or during specific functions requiring the PRRISM to
409 be pointed away from the sun. The Satellite Attitude Control & Propulsion Subsystem (ACPS) contains the hydrazine
410 thrusters to process the satellite spin axis and control its spin rate. Small orbital maneuvers are also made by these
411 thrusters. The ACPS would orient the PRRISM antenna to focus the EM wave at the entrance of the Polar Cusp to
412 redirect the solar wind for the duration of the targeting sequence. The Satellite Thermal Control Subsystem (TCS)
413 provides an acceptable thermal environment for the Satellite subsystems and instruments primarily by using passive
414 thermal control with thermal finishes and blanketing. The Satellite Attitude Determination Subsystem (ADS) is used to
415 determine the Satellite attitude and spin rate. This allows subsystems to keep within nominal environments and provide

416 a reference frame for the mission. The ADS is designed to provide knowledge of the Satellite spin axis in inertial
417 space. The PRRISM satellite would not be adding any propulsive force to the solar plasma. However, during an actual
418 targeting sequence, the EM wave would increase the laminar flow and increase proton density to increase the pressure
419 force of the solar plasma on the targeted space debris. The intercept sequence would begin with a command from
420 ground control for the Targeting Computer to access the Solar Plasma Sensor data. The Satellite Attitude
421 Determination Subsystem would orient the PRRISM to concentrate the EM wave on the solar plasma and maintain the
422 proper frame of reference for the duration of the targeting sequence. Specific to the PRRISM satellite system are the
423 Targeting Computer (TC), The Antenna EM wave Electrical Power Control Unit and the Magnetic field control unit.
424 These subsystems would interact with each other using telemetry data from the Solar Plasma Sensor; the Space Debris
425 Sensor; and the Ground Station to position the PRRISM antenna for a predetermined period. This would provide the
426 PRRISM antenna with sufficient power to produce an electromagnetic wave to redirect the solar plasma into the
427 Northern or Southern Polar Cusp with an increase in laminar flow and pressure force.

428

429 **10.2 PRRISM ENVIRONMENT**

430

431 PRRISM is a novel use of space-based assets with minimal effect on the Earth's magnetosphere and, in the near-Earth
432 orbital environment it will speed up orbital decay of debris objects. PRRISM combines the scientific research of the
433 Sun – Earth electromagnetic environment and applies proven engineering principles. PRRISM operates from an
434 elliptical orbit outside of the Polar Cusp using a controlled, focused and measured electromagnetic wave to direct a
435 narrow beam or pulse into the Polar Cusp to align the turbulent solar plasma, increase the density and match the
436 frequency and polarity of the incoming solar wind. There are limitations to reaching the low inclination orbits which
437 will have to be overcome. However, the most populated orbit is the Sun Synchronous Orbit (SSO) where satellites
438 occupying Low Earth Orbits are crossing the poles with inclinations between 80 degrees and 110 degrees. As
439 previously discussed, the small debris in Earth orbit that is not tracked and traveling at roughly 9 km/s can be more
440 lethal to satellites and humans than a larger piece that is trackable. Damage from debris is a low probability now but is
441 a high consequence event. We depend on satellites for our communications, including TV and cell phone coverage,
442 navigation, weather, disaster management, and military reconnaissance. Because PRRISM is targeting the smaller
443 debris pieces (and from outside of the debris orbit), a proportionally small increase in dynamic pressure and force will
444 be needed to remove this debris from orbit. By creating a constructive interference with the solar wind, a temporary but

445 stronger dynamic pressure could be attained at the exit of the Polar cusp. The concept relies on fine-tuning the
 446 frequency and polarity of the solar plasma in the Polar Cusp with an externally applied electromagnetic wave to
 447 incrementally increase the dynamic pressure by a small amount and create a timed 3-D intercept with the debris cloud
 448 effecting the removal and deorbit of the targeted space debris in large quantities. Many larger satellites including
 449 Skylab have been safely and successfully deorbited. However, unlike larger satellites that do not completely burn up
 450 on re-entry, the smaller pieces of debris will be destroyed during re-entry into the atmosphere. For example, using the
 451 gravimetric force equation for debris diameters between 2 cm and 200 cm, listed in Table 8, it can be shown that in a
 452 500 km orbit, the gravitational force required to maintain orbit is small for debris diameters less than 100 cm and
 453 therefore a minimum additional opposing force would be needed to slow the debris orbital speed and cause it to decay
 454 and deorbit.

455

Orbital Debris Diameter (Cm)	Gravitational Force in 500 Km orbit (Newtons)
2	0.1
10	2.2
25	17.8
50	85.4
75	213.5
100	409.1
150	1022.8
200	1959.5

456

Table 8. Gravimetric Force

457

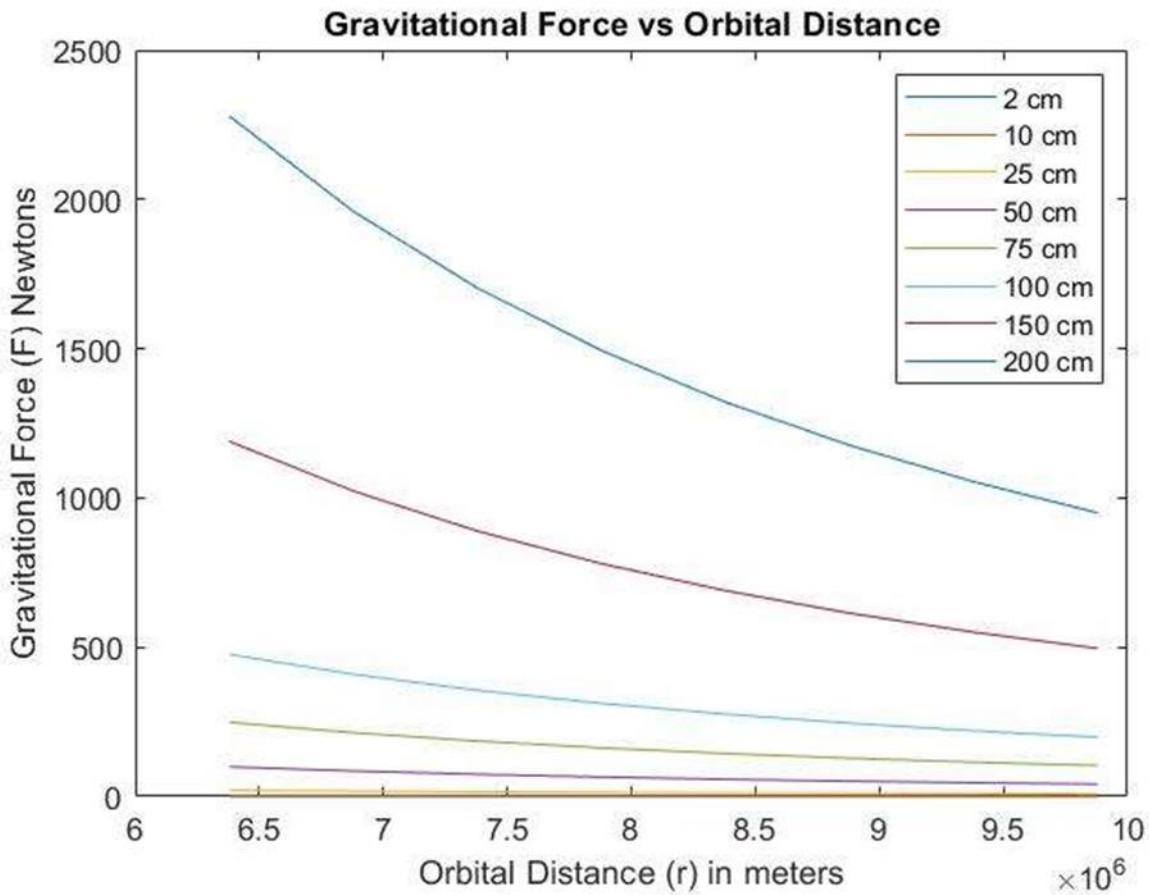
458 The gravimetric force increases with the size of the debris, and to maintain a 500 km orbit for debris less than 100 cm
 459 (213.5 Newtons for a 75cm diameter debris) the force is less than the highest estimated Polar Cusp exit force (396.6
 460 Newtons) under normal conditions (Table 9). Furthermore, a smaller opposing force could be effective in deorbiting
 461 larger debris pieces. The Polar Cusp exit force is partly determined by the exit area. Using the area based on
 462 observations by Maynard [12], the estimated exit area of the Polar cusp is calculated at $0.129 \times 10^{12} \text{ m}^2$ and is variable.
 463 This is approximately the equivalent of the combined areas of the states of Maine, New Hampshire, and Vermont. The
 464 other variable in the dynamic pressure equation is the velocity. Data from Hawkeye and IMP 8 missions [11] have
 465 shown that the velocity varies between the external cusp and the internal cusp while the density increases at altitudes
 466 below $4 R_E$. In the earlier calculations, a conservative value of 100 km/sec was used to calculate the dynamic pressure
 467 and the Polar cusp exit force. However, the solar plasma velocity and direction measured in the polar cusp during

468 science missions has a wider range from 100 to 350 km/s while moving in all directions. Table 9 shows the exit force
 469 from the polar cusp under normal conditions for these plasma velocities without any external forces applied.
 470

Plasma Velocity (Km/ sec)	Polar Cusp Exit force (Newtons) with no external forces applied
100	32.4
200	129.5
300	291.4
350	396.6

471 Table 9. Plasma Velocities

472
 473 At a velocity of 350 km/s the Polar cusp exit force is 396.6 Newtons. This is just slightly less than the force of 409.1
 474 Newtons required for a 100 cm diameter debris piece to remain in a 500 km orbit. Variations in polar cusp solar wind
 475 EM intensities, plasma velocity and plasma direction have been attributable to coronal mass injections (CME) and
 476 other solar flare activity as well as the timing and direction of the interplanetary magnetic field (IMF) when arriving at



477

478 the Earth's geomagnetic field. Utilization of PRRISM to redirect and remove debris pieces less than 100 cm in
479 diameter would require little additional EM wave energy in excess of normal conditions. EM wave energy
480 supplementation would be needed during periods of low solar cycles/ energy levels and possibly for larger pieces of
481 debris. Because of inconsistencies in mission data, additional testing would be needed for a final determination of
482 required EM wave energy. In addition, orbital decay is achievable with a fractional decrease in gravimetric force.
483 Therefore, larger pieces of debris could conceivably be removed from orbit over time using a force less than the
484 minimum gravimetric force. As shown in Plot 10, the Gravitational force decreases with higher orbits and smaller
485 debris mass. Low Earth orbital distances are between 688000 meters (1xR_E+500 km altitude) and 838000 meters
486 (1xR_E+2000 km altitude). The lighter debris particles (2 cm, 10 cm, and 25 cm) have extremely low values of
487 gravitational force throughout this orbital range. Because of the variety of space debris in both size and shape, multiple
488 solutions will be needed to resolve this growing threat to space operations. Solutions to remove large derelict satellites
489 are close to achieving success. However, these methods operate in the same orbit as the targeted debris and risk the
490 possibility of causing additional collisions that create more debris. Therefore, once the large pieces have been removed,
491 the PRRISM solution of operating outside of the debris orbit is a reasonable and safe approach to clearing the near-
492 Earth orbits. Thus, allowing safe operation for space travelers and for our commercial and government driven
493 international satellite commerce.



Clearing orbital space for a cleaner future

www.ironstarengineering.com

498

499 **11 REFERENCES**

500

- 501 1. United Nations. "Space Debris Mitigation Guidelines of the Committee on the Peaceful Uses of Outer Space",
502 United Nations Office for Outer Space Affairs, Interagency Space Debris Coordination Committee (IADC),
503 resolution 62/217, Dec 22, 2007.
- 504
- 505 2. National Aeronautics and Space Administration. "Orbital Debris Environment for Spacecraft Designed to
506 Operate in Low Earth Orbit", NASA Technical Memorandum 100471.

- 507
- 508 3. Weeden, B. and Shortt, K. “*Development of in Architecture of Sun-Synchronous Orbital Slots to Minimize*
509 *Conjunctions*” in SpaceOps 2008 conference, Paper AIAA 2008-3547.
- 510
- 511 4. Boain, R.J. “*A-B-Cs of Sun-Synchronous Orbit Mission Design*” in *14th AAS/AIAA Space Flight Mechanics*
512 *conference*, Maui, Hawaii, 2004, Paper AAS 04-108.
- 513
- 514 5. Oltrogge, D. and Kelso, T.S. “*Getting to know our Space Population from the Public Catalog*”, Analytic
515 Graphics Incorporated (AGI), Center for Space Standards and Innovation, Paper AAS 11-416.
- 516
- 517 6. Schwenn, R. "Solar Wind: Global Properties", *Encyclopedia of Astronomy and Astrophysics*, Edited by Paul
518 Murdin, article id. 2301, Bristol: Institute of Physics Publishing, Nov 2000. Available:
519 <http://eaa.iop.org/abstract/0333750888/2301>
- 520
- 521 7. Korth, A., et al, “*The response of the polar cusp to a high-speed solar wind stream studied by a multi-spacecraft*
522 *wavelet analysis*”, J. of Atmospheric and Solar-Terrestrial-physics, Vol 73, pp52-60, Elsevier Ltd, October 2011
- 523
- 524 8. Gurnett, D.A. and Frank, L.A., “*Plasma Waves in the Polar Cusp: Observations from Hawkeye 1*”, *Journal of*
525 *Geophysical Research*, vol. 83, no. A4, pp. 1447-1462, Apr 1978
- 526
- 527 9. Orfanidis, S.J., *Electromagnetic waves and Antennas*. Rutgers University, Aug 2016
- 528
- 529 10. Borofsky, J.E. “*The spatial structure of the oncoming solar wind at Earth and the shortcomings of a solar-wind*
530 *monitor at LI*”, J. of Atmospheric and Solar-Terrestrial Physics, Vol 177, pp 2-11, Elsevier Ltd, 2018
- 531
- 532 11. Chen, S.H., et al, “*Exterior and interior polar cusps: Observations from Hawkeye*”, *J. of Geophysical Research*,
533 vol. 102, no. A6, pp 11,335-11,347, Jun 1, 1997, American Geophysical Union, Jun 1997
- 534

- 535 12. Maynard, N.C., "*Coupling the Solar-Wind/IMF to the Ionosphere Through the High Latitude Cusps*", *Surveys*
536 *in Geophysics*, (2005) 26:255-280, Springer 2005
537
- 538 13. Peterson, W.K., et al, "*Sources of plasma in the high altitude cusp*", *J. Of Atmospheric and Solar-Terrestrial*
539 *Physics*, Vol 87-88, pp1-10, Elsevier Ltd, 2011